ACS APPLIED MATERIALS & INTERFACES

RESEARCH ARTICLE

www.acsami.org

Effect of Polymer Aggregation on the Open Circuit Voltage in Organic Photovoltaic Cells: Aggregation-Induced Conjugated Polymer Gel and its Application for Preventing Open Circuit Voltage Drop

Bong-Gi Kim,[†] Eun Jeong Jeong,[‡] Hui Joon Park,[†] David Bilby,[‡] L. Jay Guo,[†,§] and Jinsang Kim*[,†,‡,⊥]

[†]Macromolecular Science and Engineering, [‡]Department of Materials Science and Engineering, [§]Electrical Engineering and Computer Science, [⊥]Chemical Engineering, University of Michigan, Ann Arbor, Michigan 48109, United States

ABSTRACT: To investigate the structure-dependent aggregation behavior of conjugated polymers and the effect of aggregation on the device performance of conjugated polymer photovoltaic cells, new conjugated polymers (PVTT and CN-PVTT) having the same regioregularity but different intermolecular packing were prepared and characterized by means of UV−vis spectroscopy and atomic force microscopy (AFM). Photovoltaic devices were prepared with these polymers under different polymer-aggregate conditions. Polymer aggregation induced by thermal annealing increases the short circuit current but provides no advantage in the overall power conversion efficiency because of a decrease in the open circuit voltage. The device fabricated from a pre-aggregated polymer suspension, acquired from ultrasonic agitation of a conjugated polymer gel, showed enhanced performance because of better phase separation and reduced recombination between polymer/PCBM.

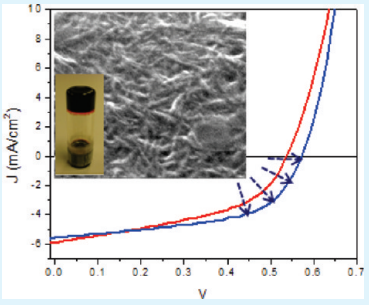

KEYWORDS: self-assembly, organic photovoltaic cells, conjugated polymers, nanowires, organic electronics

INTRODUCTION

The aggregation behavior of conjugated polymers (CPs) has drawn considerable attraction because of its effect on the optical and the electronic properties of the CPs in the solid state.[1−13] CPs show an increased absorption coefficient,[8,9] an unusual absorption or emission shift,[10,11] or the appearance of a new absorption peak[5,8,12,13] because of aggregation. Also, it has been reported that the aggregation of CPs improves carrier mobility, promising improvements for organic thin-film transistors (OTFTs)[14−16] and organic photovoltaic devices.[17−31] For instance, poly(3-hexylthiophene) (P3HT) and analogous polymers exhibited much faster hole mobility, and therefore more efficient photovoltaic devices, when aggregation was induced by thermal annealing[29] or solvent-assisted annealing methods.[27] The driving force causing aggregation in CPs, however, has not been fully described. Previously reported results indicate that regioregular (RR) side chains or strong aromatic interactions between polymer backbones are helpful for aggregation;[8,32] higher RR P3HT shows stronger aggregation behavior and polymers having a relatively planar conjugated backbone frequently exhibit aggregation via aromatic interactions.

Recently, the origin of the open circuit voltage (V_{oc}) in CP/PCBM blend solar cells was investigated by analyzing the degree of charge transfer interactions between CPs and PCBM.[33] CPs having better aggregation behavior interacted more strongly with PCBM and produced relatively lower V_{oc} (compared to the theoretical value determined by the optical band gap between the HOMO of the donor and the LUMO of the acceptor) because of increased recombination.[34] In other words, although a strongly aggregating CP provides better charge mobility, the photovoltaic performance cannot be optimized unless recombination is suppressed to obtain a high V_{oc}.

In this contribution, we have designed and synthesized two new CPs and have investigated the influence of their structure on aggregation properties and on solar cell efficiency. The two polymers, with the same side chains and conjugated backbone, only differ with the inclusion of a bulky cyano group at the vinylene moiety to control their aggregation behavior. We observed an aggregation-induced gelation from the CP without the bulky cyano group and then, by applying ultrasonication to breakup the polymer gel, pre-assembled conjugated polymer fibers could be prepared for photovoltaic device fabrication (similar to how we handled P3HT in our previous work).[35] The device performance, particularly the open circuit voltage and the short circuit current density, was systematically investigated and related to the aggregated structure of the CPs. In addition, the dark saturation current density (J_0) value was calculated to estimate the degree of recombination in each photovoltaic device. On the basis of these efforts, we suggest an improved device fabrication condition for highly crystalline CPs.

EXPERIMENTAL SECTION

Materials. All starting materials were purchased from commercial suppliers (Aldrich and Fisher Sci.). Synthesized compounds were fully characterized with ^{1}H NMR and GC-mass, and molecular weights of the

Received: August 18, 2010
Accepted: January 5, 2011

   dx.doi.org/10.1021/am101067x | ACS Appl. Mater. Interfaces XXXX, XXX, 000–000

Scheme 1. Chemical Structures and Synthetic Routes of the Polymers[a]

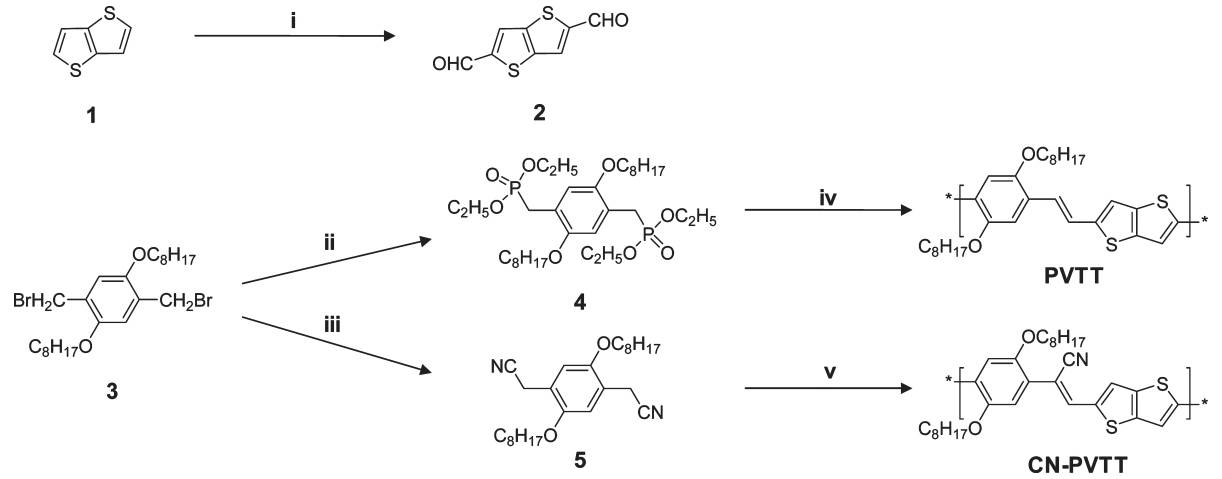

[a] (i) BuLi, DMF, THF, -75 °C; (ii) triethylphosphite, 90°C; (iii) NaCN, DMF, reflux; (iv) 2, KOtBu, DMF, 80°C; (v) 2, KOtBu, THF, KtBuOH, 70 °C.

final polymers were measured with gel permeation chromatography (GPC) relative to polystyrene calibration standards.

Thieno[3,2-b]thiophene-2,5-dicarbaldehyde (2). Under argon, 2.5 M n-BuLi in n-hexane (6.27 ml, 15.69 mmol) was slowly added to a solution of thieno[3,2-*b*]thiophene (1g, 7.13 mmol) in dry diethyl ether (20 mL) at −75 °C. After stirring the solution for 30 min at -75°C, anhydrous DMF (1.21 ml) was added and the mixture was warmed to room temperature while stirring overnight. The white solid was filtered off and was washed with water, methanol and diethyl ether several times sequentially. Obtained white powder (0.91 g, 65%) was used without further purification for polymerization. Not sufficiently soluble for NMR analysis and *m*/*z* EIMS 196.

2,5-Di-*n*-octyloxy-1,4-xylene-diethylphosphonate ester (4). Triethylphosphite (10.25 g, 61.68 mmol) and 2,5-di-*n*octyloxy-1,4-bis(bromomethyl)benzene (**3**) (4.15 g, 7.98 mmol) were heated to 90 °C for 16 h. After removing excess triethylphosphite by vacuum distillation, n-hexane (25 ml) was added and the mixture was stirred at 50 °C for 30 min. The mixture was recrystallized from petroleum ether after solvent evaporation and pale yellow crystals were obtained (3.65 g, 72.0%). ^{1}H NMR ($CDCl_3$, ppm): 6.92 (s, 2H), 4.02 (qua, 8H), 3.92 (t, 4H), 3.28 (d, 4H) 1.77 (qui, 4H), 1.29-1.24 (m, 32H), 0.89 (t, 6H).

(4-(Cyanomethyl)-2,5-bis(*n*-octyloxy)phenyl)acetonitrile (5). After dissolving 1,4-bis(bromomethyl)-2,5-bis-(*n*-octyloxy) benzene (**3**) (1.0 g, 1.92 mmol) in 25 ml of anhydrous DMF, NaCN (0.235 g, 4.8 mmol) was added. The mixture was refluxed overnight and cooled to room temperature before pouring it into 50 mL of NaOH (0.5 M solution in water). The solid product was filtered off, washed with methanol several times, redissolved in chloroform, washed with brine, and purified by recrystallization from ether/chloroform (0.41 g, 52%). ^{1}H NMR ($CDCl_3$, ppm): 6.92 (s, 2H), 3.95 (tri, 4H), 3.92 (t, 4H), 3.69 (s, 4H), 1.29-1.24 (m, 24H), 0.89 (t, 6H).

PVTT. A solution of (**4**) (1g, 1.575 mmol) and (**2**) (0.309g, 1.575 mmol) in DMF was heated to 80°C. Potassium *tert*-butoxide (KOtBu) (0.47 g, 4.19 mmol) was added at once. The reaction mixture was stirred at 80°C for 4 h and then poured into water (100 mL). Reddish solid was filtered off, washed with water and methanol several times. After redissolving solid into chloroform by heating, it was precipitated with methanol. Finally, residual monomers or oligomers were removed by Soxhlet extraction with methanol for 24 h (M_w 28 000; PDI 1.6).

CN-PVTT. To a solution of (**5**) (1 g, 2.424 mmol) and (**2**) (0.475 g, 2.424 mmol) in anhydrous THF (100 mL) and tert-butanol (100 mL) was added potassium *tert*-butoxide (0.544 g), and the mixture was heated to 70°C for 2 h. After cooling down to room temperature, it was poured into water and acidified with HCl. The purple color solid was filtered off and washed with water and methanol several times. After redissolving solid into chloroform by heating, it was precipitated with methanol. Finally, residual monomer and oligomers were removed by Soxhlet extraction with methanol for 24 h (M_w 22 000; PDI 2.2).

Fabrication and Characterization of Photovoltaic Device. PCBM[70] was purchased from SES research and used without further purification. After dissolving polymers (10 mg) and PCBM-[70] (40 mg) in *o*-dichlorobenzene (1.5 ml), the obtained solutions were filtrated with a PTFE syringe filter having 0.45 μm pore and used to form the active layer by means of spin-casting. The PVTT gel was made by dissolving 10 mg of PVTT in 0.9 mL of *o*-dichlorobenzene and keeping the solution for one day under ambient conditions. Obtained gel was treated with ultrasonication at room temperature for 5 min and blended with chlorobenzene (0.9 mL) containing PCBM[70] (40 mg). The resulting blend solution was used for a similar characterization. ITO-coated glass was cleaned with acetone and IPA followed by UV ozone treatment for 5 min. PEDOT:PSS (Baytron PH 500) was spin-cast on the substrate and baked at 150 °C for 15 min. Different polymer/PCBM[70] blend solutions were spin-cast at 1000 rpm for 30 s. The thermally annealed samples were annealed for 10 min at 150 °C, and nonannealed samples were dried of solvent for 50 minutes at 60 °C. Final devices were fabricated by depositing a 1 nm thick LiF and a 70 nm Al layer (9.6 mm^2) sequentially under 5×10^{-7} Torr. All devices were characterized under ambient conditions and the typical illumination intensity was 100 mW/cm^2 (AM 1.5G Oriel solar simulator).

Hole-Only Device. Hole-only devices were fabricated; molybdenum oxide (MoO_3, 20 nm) was deposited on top of the 100 nm thick PVTT/PCBM[70] active layers, replacing the LiF layer of previous photovoltaic devices, to block electron injection from aluminum.

RESULTS AND DISCUSSION

The detailed synthetic procedure for the CPs investigated in this study is shown in Scheme 1. Thieno[3,2-*b*]thiophene (**1**) and 1,4-bis(bromomethyl)-2,5-bis(octyloxy)benzene (**3**) were prepared as previously described.[36,37] The Arbuzov reaction with (**3**) yielded 2,5-di-*n*-octyloxy-1,4-xylenediethylphosphonate ester (**4**),[38] and sodium cyanide is used to result in (4-(cyanomethyl)-2,5-bis(*n*-octyloxy)phenyl)acetonitrile (**5**).[39] Thieno[3,2-b]thiophene-2,5-dicarbaldehyde (**2**)[40] produced from (**1**) by lithiation of the appropriate position with

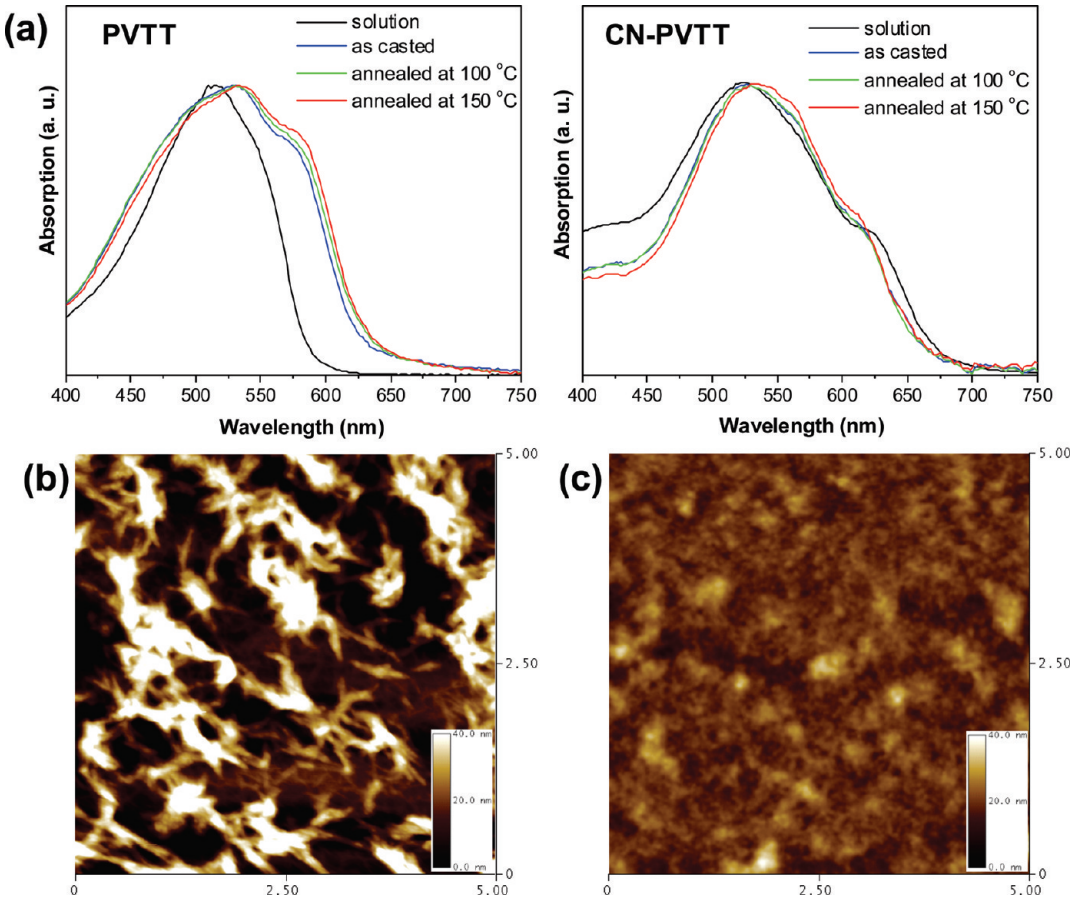

Figure 1. Aggregation behaviors of PVTT and CN-PVTT. (a) UV−vis absorption of solution ($CHCl_3$) and film fabricated under different annealing conditions. Tapping mode AFM image (height, 5μm × 5μm) after annealing at 150 °C (b) PVTT, and (c) CN-PVTT.

buthyllithium (BuLi) in anhydrous tetrahydrofuran (THF) followed by formylation with *N*,*N*-dimethyl formamide (DMF) under an argon atmosphere. The final polymers, PVTT and CN-PVTT, were prepared from a Knoevenagel condensation using potassium *tert*-butoxide.

The aggregation behavior of the synthesized polymers was first characterized with UV−vis absorption spectroscopy both in chloroform solution and of dried films. The dried films were prepared by spin-casting from solutions of the polymers (10 mg) in *o*-dichlorobenzene (0.9 mL). As shown in Figure 1a, dried films of PVTT exhibit a new absorption peak around 575 nm (compared to the solution absorption) which becomes stronger when thermally treated for 10 min. On the contrary, CN-PVTT shows exactly the same absorption pattern regardless of the sample preparation conditions and exhibits red-shifted absorption compared to PVTT because of intramolecular charge transfer between electron withdrawing CN and electron donating aromatic groups.[41] We believe that the different absorption phenomena in PVTT and CN-PVTT in the solid state are due to the presence and absence of aggregation, as demonstrated by a morphological study of the thermally treated dried films with tapping mode AFM. In Figure 1b, PVTT displays a strong fibrous network when annealed at 150 °C, but under similar conditions, CN-PVTT shows a smoother morphology without any specific features (Figure 1c), indicating that no appreciable aggregation occurs. The totally different aggregation behavior in PVTT and CN-PVTT can be similarly attributed to the effect of the cyano group in CN-PVTT, as reported in an analogous small molecule system.[42] Unlike the relatively planar conformation of the stillbene unit of PVTT, the bulky cyano group attached to the vinylene moiety of CN-PVTT sterically prevents aggregation which would otherwise be driven by the aromatic interaction between the polymer's conjugated backbones. It is apparent that aromatic $\pi-\pi$ interactions still play an important role in promoting polymer aggregation despite the generally low crystallinity of polymers compared to analogous monomers or oligomers.

Interestingly, when kept under ambient conditions for a day, a PVTT solution, with the same composition used for preparing dried films for the UV−vis study, turned into a polymer gel as depicted in Figure 2a. This gel showed reversible feature; by heating, it became the original clear solution and after one day it reverted to the organic gel. The driving force for this gelation behavior can be traced from the strong aggregation characteristics of PVTT; because it does not contain any functional groups for secondary bonding, only aromatic $\pi-\pi$ interaction between polymer backbones can contribute to the aggregation and gelation. The surface morphology, after drying the obtained gel, was analyzed using scanning electron microscopy (SEM), and we found tiny particlelike spheres (200−250 nm) and a fibrous network (20−25 nm) as shown in Figure 2b. Macroscopically, the PVTT organic gel seems to result from the entanglement of fibers which propagate from the particlelike spheres. To obtain a homogeneous PVTT suspension, we sonicated the PVTT gel for 5 min. The resulting suspension was spin-cast to investigate the film morphology. As shown in

dx.doi.org/10.1021/am101067x |*ACS Appl. Mater. Interfaces* XXXX, XXX, 000–000

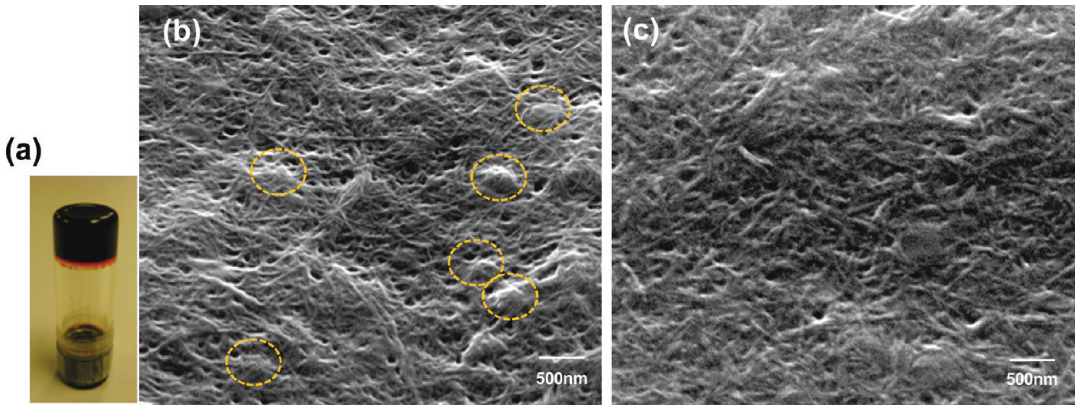

Figure 2. (a) PVTT gel in *o*-dichlorobenzene. SEM images: (b) gel after drying (circles indicate particle-like spheres), and (c) film after spin-casting with ultra-sonicated PVTT gel suspension.

Table 1. Device Performance of Photovoltaic Cells Made of Polymer/PCBM[70] in Different Conditions

	PVTT			CN-PVTT
polymers	nonannealed	150 °C for 10 min	suspension (nonannealed)	150 °C for 10 min
J_{sc} (mA/cm^2)	−4.92	−5.91	−5.55	−0.09
V_{oc} (V)	0.57	0.54	0.57	0.61
FF	0.53	0.46	0.55	0.21
PCE (%)	1.49	1.46	1.76	0.01
hole mobility (m^2/(V s))	2.44×10^{-10}	3.64×10^{-9}	5.75×10^{-10}	1.49×10^{-15}
J_0 (mA/cm^2)	8.25×10^{-10}	4.44×10^{-9}	9.92×10^{-10}	5.08×10^{-12}

Figure 2c, the film made from the ultrasonicated PVTT gel suspension exhibited more uniform features consisting of fibrous-shaped PVTT pre-aggregates. Also, the particlelike PVTT aggregates that were observed in the bulk PVTT gel seemed to have mostly disappeared after the ultrasonic treatment. Obtained suspension was used for photovoltaic device fabrication after blending with PCBM, (the pre-aggregated portion of the PVTT suspension was about 62% by weight).

The HOMO levels of PVTT and CN-PVTT were measured with cyclic voltammetry using thin films prepared from *o*-dichlorobenzene (5 mg/mL). $Ag/AgNO_3$ served as the pseudo reference electrode, ferrocene was used for calibration, and the supporting electrolyte was tetrabutylammonium hexafluorophosphate (0.1 M) in acetonitrile. LUMO levels were then calculated based on the absorption onset of the UV-vis spectrum; the HOMO/LUMO values of PVTT and CN-PVTT were −4.85 eV/−2.89 eV and −5.49 eV/−3.65 eV, respectively. Because these energy levels were well-matched with the HOMO/LUMO values of PCBM[70], an electron acceptor for photovoltaic applications, we investigated photovoltaic device performance after dissolving polymers/PCBM[70] (1/4) into *o*-dichlorobenzene and spin-casting 100 nm thick films.

Photovoltaic device performance was investigated under AM 1.5G conditions after depositing 1 nm LiF and 70 nm Al top electrode layers having an island geometry to prevent overestimation.[43] As summarized in Table 1, we fabricated multiple devices (more than 50 devices under each condition) with PVTT and CN-PVTT, and their photovoltaic device performance was compared after thermal annealing (because CN-PVTT did not show any meaningful current value without thermal treatment). Thermally annealed and nonannealed samples were obtained by drying for 10 min at 150°C and for 50 min at 60°C, respectively. Even after thermal annealing was applied, CN-PVTT exhibited a much lower J_{sc} value (0.09 mA/cm^2) compared to the PVTT based device (5.91 mA/cm^2), which could be attributed to the much lower hole mobility of CN-PVTT (Table 1 and Figure 4a). We believe that the poor aggregation behavior and the electron-withdrawing nitrile moiety of CN-PVTT cause the low hole mobility by increasing the series resistance[44,45] and by acting as a hole trapping site,[46] respectively. In addition, the CN-PVTT/PCBM blend film did not exhibit a phase separated mophology (required for effective device function), but rather, it has a smooth, continuous, and featureless surface (Figure 5d). This implies that the percolation pathways, required for efficient charge carrier transport, are not appropriately generated in the CN-PVTT/PCBM blend film.

Thermal annealing of PVTT enhanced the short circuit current density (J_{sc}) by strengthening polymer aggregation, thus facilitating carrier transport. However, the decreased V_{oc} and fill factor (FF) ultimately caused poor performance compared to the non-annealed device. As shown in Figure 3b, thermal annealing increased the absorption intensity around 575 nm, indicating the formation of aggregation. In addition, the hole mobility increases by 15 times from 2.44×10^{-10} m^2 V^{-1} s^{-1} to 3.64×10^{-9} m^2 V^{-1} s^{-1} after the thermal annealing. The hole mobilities were calculated by applying the space-charge limited current (SCLC) model at low voltages (Figure 4a).[45] To investigate the decreased FF and the relatively low V_{oc} after thermal annealing in the PVTT based photovoltaic devices, we characterized the morphology of active layers (PVTT/PCBM-[70]) under tapping mode AFM. Additionally, we extracted the dark saturation current density (J_0) values from the $J-V$ curves in

dx.doi.org/10.1021/am101067x |ACS Appl. Mater. Interfaces XXXX, XXX, 000–000

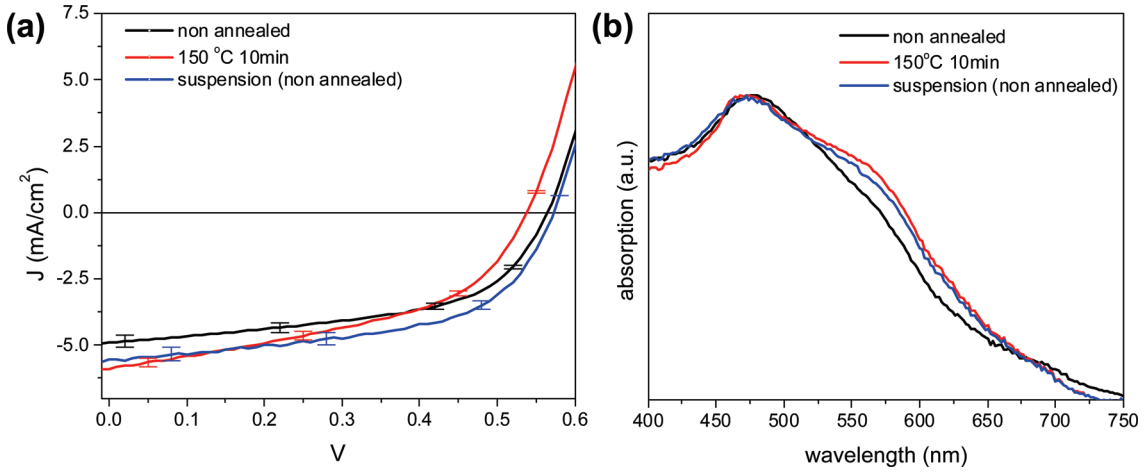

Figure 3. (a) $J-V$ curves of PVTT/PCBM[70] blend systems, (b) UV−vis absorption of fabricated devices.

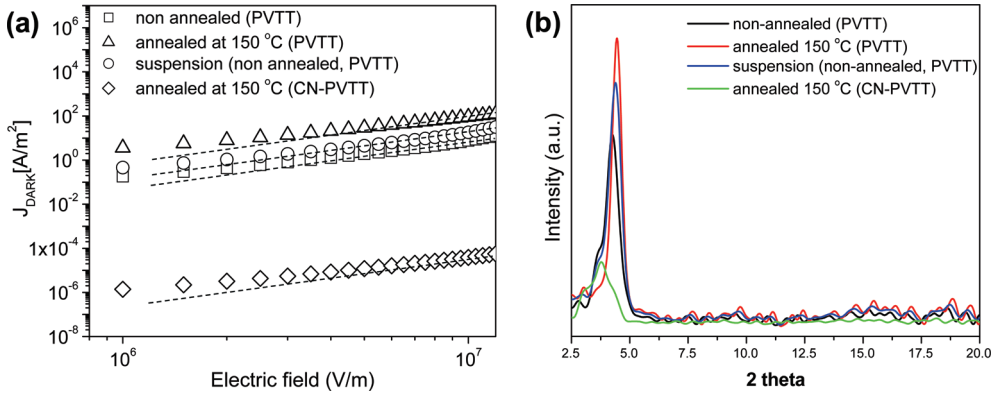

Figure 4. (a) Measured $J-E$ characteristics under dark conditions for hole-only photovoltaic devices. The solid lines represent the linear fit of the experimental data using the SCLC model. (b) X-ray diffraction patterns of the obtained polymer/PCBM blends.

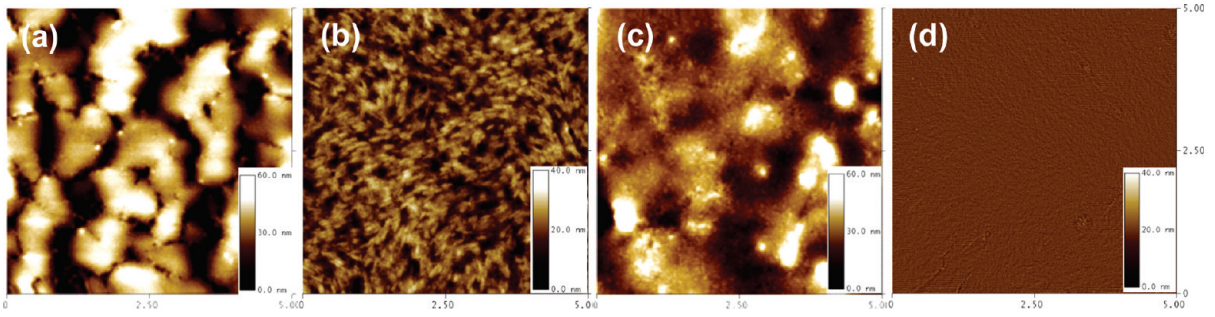

Figure 5. Tapping mode AFM images (height, 5μm × 5 μm) of PVTT/PCBM[70] films. (a) non-thermal-annealed film, b) thermal-annealed film at 150 °C, (c) non-thermal-annealed film made from the ultrasonicated PVTT gel suspension, and (d) thermal annealed CN-PVTT/PCBM[70] at 150 °C.

a previously described manner.[33] Because J_0 is dominated by recombination, it can explain the variations of the V_{oc} in organic photovoltaic devices having different materials and/or morphologies.[47] As depicted in images a and b in Figure 5, nonannealed films showed rougher morphologies than thermally annealed films. The calculated root mean square (RMS) roughness decreased from 4.72 to 2.24 nm during the thermal annealing procedure. In addition, considering that the bright, polymer-rich domain formed into a relatively large feature in Figure 5a, we speculate that the nonthermally annealed condition gives a well phase-separated morphology between the polymer and PCBM[70]. This mild drying condition (50 min at 60 °C) allows enough time for the formation of polymer-rich domains. However, the thermally annealed film showed poor phase separation with islandlike or cul-de-sac domains. We believe that this poor PVTT/PCBM[70] phase separation is due to the high annealing temperature (150 °C), which leads to fast solvent evaporation that restricts the mobility of the blend film. To verfy the influence of morphology on recombination, we characterized the devices with X-ray diffraction (XRD) and morphological data

dx.doi.org/10.1021/am101067x |ACS Appl. Mater. Interfaces XXXX, XXX, 000–000

were compared to their calculated J_0 values. As shown in Figure 4b and Table 1, thermal annealing made PVTT/PCBM films adopt a more closely packed structure evidenced by the intensified diffraction peak at $2\theta = 4.45°$. The annealed, more tightly packed films also exhibited an increased J_0 (from 8.25×10^{-10} before annealing to 4.44×10^{-9} afterwards). This implies that thermal annealing facilitates charge recombination between PVTT and PCBM, resulting in the decreased V_{oc}. The smaller domains, which lead to a larger donor/acceptor interface area (Figure 5b), and the stronger PVTT aggregation character, which increases intermolecular interaction between PVTT and PCBM, as similarly described both in small molecule and polymer systems,[47,48] could be ascribed as the main factors that induce higher recombination in the thermally annealed device. In nonannealed PVTT/PCBM blend films, aggregated and nonaggregated structures coexist; XRD shows both strong diffraction ($2\theta = 4.24°$), like the thermally annealed films, and a weak broad diffraction ($2\theta = 3.73°$), like the nonaggregated CN-PVTT/PCBM films. These differences in morphology and in the degree of recombination explain the higher fill factor (FF) of the nonannealed devices because the island domains and the strong recombination (larger J_0) in the thermally annealed device play a role as possible carrier traps resulting in the decreased shunt resistance and smaller FF.[49] On the basis of the results from these devices fabricated under different annealing conditions, we conclude that controlling the degree of polymer aggregation in the active layer of photovoltaic devices is important to obtain higher current densities and to prevent V_{oc} decrease.

Spin-casting from the ultra-sonicated PVTT suspension (from the PVTT gel) was studied as a route to an aggregation optimized fabrication condition. We obtained a blend solution of ultrasonicated PVTT gel suspension/PCBM[70] by mixing the ultrasonicated PVTT gel suspension and a PCBM[70] solution (40 mg dissolved into 0.9 ml of chlorobenzene). The additional chlorobenzene did not break the suspended PVTT state because it was not a particularly good solvent for PVTT. The device made from the ultrasonicated PVTT gel suspension was characterized under the same conditions as the nonthermally annealed PVTT/PCBM[70] device. As we expected, the device adopting the PVTT preaggregates exhibited better J_{sc} values than the device fabricated using the PVTT gel solution and yet maintains similar V_{oc} values. As shown in Figure 4a, the device made of the PVTT suspension exhibited a hole mobility (5.75×10^{-10} $m^2 V^{-1} s^{-1}$) more than two times larger than that made from the nonthermally annealed PVTT solution. In addition, the film showed similar inter-chain packing ($2\theta = 4.36$ and $3.73°$) and morphology (RMS ~4.86 nm) with the nonthermally treated film except displaying tiny fibrous aggregates in the polymer-rich bright domains, indicating preaggregate formation from the PVTT ge1 suspension (Figure 5c). The enhanced device efficiency is likely due to the combined effects of the preaggregate and nonaggregated parts of the PVTT suspension. The preaggregate contributes a mobility enhancement leading to a better J_{sc} and the non-aggregated part (existing around aggregated PVTT domains) prevents a V_{oc} drop. The nonaggregated part helps suppress recombination by acting similar to the non-thermally annealed PVTT/PCBM[70] device in terms of donor/acceptor interaction and film morphology (Table 1 and Figure 5). On the basis of the photovoltaic device work with PVTT, we suggest that an optimized fabrication condition for better device performance involves spin-casting from a fibrous CP suspension to form polymer domains composed of aggregated core and nonaggregated shell units, similar to those described in P3HT fiber/PCBM based devices.[50]

CONCLUSION

In summary, we synthesized two novel conjugated polymers, PVTT and CN-PVTT, having the same side chains and conjugated backbone. Their aggregation behaviors were investigated by UV−vis spectroscopy, XRD, and AFM studies. PVTT showed strong aggregation properties, but CN-PVTT did not display aggregation because of its bulky cyano group, which prevents aromatic interactions between polymer backbones. The strong aggregation behavior of PVTT resulted in a self-assembled polymer gel in *o*-dichlorobenzene and its morphology was investigated by means of SEM and AFM; we found tiny particle-like cores surrounded by a fibrous network. Photovoltaic cells based on PVTT/PCBM[70] were fabricated from homogeneous solutions and with the self-assembled PVTT suspensions from the gel, and their device performance was compared and analyzed in connection with the AFM and UV-Vis results. PVTT-based devices without thermal treatment showed better V_{oc}, FF, and power conversion efficiency than thermally treated samples. In our polymer system, thermal annealing did not give a fully phase separated PVTT/PCBM morphology, which has negative effects on the overall device efficiency. To optimize the device morphology/performance, we spin-cast from a PVTT ge1 suspension containing preassembled polymer fibers obtained from ultrasonic treatment to a PVTT gel. The ultra-sonicated PVTT gel enhanced current in photovoltaic devices without losing V_{oc}. Fabricating organic solar cells from a preassembled polymer suspension is a promising tool to increase the overall power conversion efficiency by preventing V_{oc} decreases in polymer systems having a strong aggregation tendency.

AUTHOR INFORMATION

Corresponding Author
*E-mail: jinsang@umich.edu.

ACKNOWLEDGMENT

This material is based upon work supported as part of the Center for Solar and Thermal Energy Conversion in Complex Materials, and Energy Frontier Research Center funded by the U. S. Department of Energy, Office of Science, Office of Basic Energy Sciences under Award Number (DE-SC0000957). B.-G. Kim was also partly supported by Michigan Memorial Phoenix Energy Institute (MMPEI) fellowship.

REFERENCES

(1) Shi, Y.; Liu, J.; Yang, Y. *J. Appl. Phys.* **2000**, *87*, 4254.
(2) Nguyen, T.-Q.; Martini, I. B.; Liu, J.; Schwartz, B. J. J. *Phys. Chem. B.* **2000**, *104*, 237.
(3) Sirringhaus, H.; Brown, P. J.; Friend, R. H.; Nielsen, M. M.; Bechgaard, K.; Langeveld-Voss, B. M. W.; Spiering, A. J. H.; Janssen, R. A. J.; Meijer, E. W.; Herwig, P.; de Leeuw, D. M. *Nature* **1999**, *401*, 685.
(4) Cornil, J.; dos Santos, D. A.; Crispin, X.; Silbey, R.; Brédas, J. L. *J. Am. Chem. Soc.* **1998**, *120*, 1289.
(5) Kim, J.; Swager, T. M. *Nature* **2001**, *411*, 1030.
(6) Kim, J.; Levitsky, I. A.; McQuade, D. T.; Swager, T. M. *J. Am. Chem. Soc.* **2002**, *124*, 7710.

(7) Tammer, M; Monkman, A. P. *Adv. Mater.* **2002**, *14*, 210.
(8) Kim, Y.; Cook, S.; Tuladhar, S. M.; Choulis, S. A.; Nelsonm, J.; Durrant, J. R.; Bradley, D. C.; Giles, M.; Mcculloch, I.; Ham, C.-S.; Ree, M. *Nat. Mater.* **2006**, *5*, 197.
(9) Losurdo, M.; Giangregorio, M. M.; Capezzuto, P.; Cardone, A.; Martinelli, C.; Farinola, G. M.; Babudri, F.; Naso, F.; Büchel, M.; Bruno, G. *Adv. Mater.* **2009**, *21*, 1115.
(10) Hsu, J.-H.; Fann, W.; Tsao, P.-H.; Chuang, K.-R.; Chen, S.-A. *J. Phys. Chem. A* **1999**, *103*, 2375.
(11) Nilsson, K. P. R.; Rydberg, J.; Baltzer, L.; Inganas, O. *Proc. Natl. Acad. Sci. U.S.A.* **2003**, *100*, 10170.
(12) Osaka, I.; Sauvé, G.; Zhang, R.; Kowalewski, T.; McCullough, R. D. *Adv. Mater.* **2007**, *19*, 4160.
(13) Samorí, P.; Francke, V.; Müllen, K.; Rabe, J. P. *Chem. Eur. J.* **1999**, *5*, 2312.
(14) Mcculloch, I.; Heeney, M.; Bailey, C.; Genevicius, K.; Macdonald, I.; Shkunov, M.; Sparrowe, D.; Tierney, S.; Wanger, R.; Zhang, W.; Chabinyc, M. L.; Kline, R. J.; Mcgehee, M. D.; Toney, M. F. *Nat. Mater.* **2006**, *5*, 328.
(15) Qui, L.; Lee, W. H.; Wang, X.; Kim, J. S.; Lim, J. A.; Kwak, D.; Lee, S.; Cho, K. *Adv. Mater.* **2009**, *21*, 1349.
(16) Murphy, A. R.; Liu, J.; Luscombe, C.; Kavulak, D.; Fréchet, J. M. J.; Kline, R. J.; McGehee, M. D. *Chem. Mater.* **2005**, *17*, 4892.
(17) Li, G.; Shrotriya, V.; Huang, J.; Yao, Y.; Moriarty, T.; Emery, K.; Yang, Y. *Nat. Mater.* **2005**, *4*, 864.
(18) Hoth, C. N.; Schilinsky, P.; Choulis, S. A.; Brabec, C. J. *Nano Lett.* **2008**, *8*, 2806.
(19) Park, S. H.; Roy, A.; Beaupre, S.; Cho, S.; Coates, N.; Moon, J. S.; Moses, D.; Leclerc, M.; Lee, K.; Heeger, A. J. *Nat. Photonics* **2009**, *3*, 297.
(20) Schilinsky, P.; Asawapirom, U.; Scherf, U.; Biele, M.; Brabec, C. J. *Chem. Mater.* **2005**, *17*, 2175.
(21) Peet, J.; Kim, J. Y.; Coates, N. E.; Ma, W. L.; Moses, D.; Heeger, A. J.; Bazan, G. C. *Nature Mater.* **2007**, *6*, 497.
(22) Padinger, F.; Rittberger, R. S.; Sariciftci, N. S. *Adv. Funct. Mater.* **2003**, *13*, 85.
(23) Riedel, M.; Dyakonov, V. *Phys. Status Solidi A* **2004**, *201*, 1332.
(24) Yang, X.; Loos, J.; Veenstra, S. C.; Verhees, W. J. H.; Wienk, M. M.; Kroon, J. M.; Michels, M. A. J.; Janssen, R. A. J. *Nano Lett.* **2005**, *5*, 579.
(25) Kim, Y.; Choulis, S. A.; Nelson, J.; Bradley, D. D. C.; Cook, S.; Durrant, J. R. *Appl. Phys. Lett.* **2005**, *86*, 063502.
(26) Li, G.; Shrotriya, V.; Yao, Y.; Yang, Y. *J. Appl. Phys.* **2005**, *94*, 043704.
(27) Li, G.; Shrotriya, V.; Huang, J.; Mariarty, T.; Emery, K.; Yang, Y. *Nat. Mater.* **2005**, *4*, 864.
(28) Reyes-Reyes, M.; Kim, K.; Carroll, D. L. *Appl. Phys. Lett.* **2005**, *87*, 083506.
(29) Ma, W.; Yang, C.; Gong, X.; Lee, K.; Heeger, A. J. *Adv. Funct. Mater.* **2005**, *15*, 1617.
(30) White, M. S.; Olson, D. C.; Shaheen, S. E.; Kopidakis, N.; Ginley, D. S. *Appl. Phys. Lett.* **2006**, *89*, 143517.
(31) Hoppe, H.; Sariciftci, N. S. *J. Mater. Chem.* **2006**, *16*, 45.
(32) Samorí, P.; Francke, V.; Müllen, K.; Rabe, J. P. *Chem. Eur. J.* **1999**, *5*, 2312.
(33) Vandewal, K; Tvingstedt, K; Gadisa, A; Inganas, O; Manaca, J. M. *Nat. Mater.* **2009**, *8*, 904.
(34) Yang, L.; Zhou, H.; You, W. *J. Phys. Chem. C* **2010**, *114*, 16793.
(35) Kim, B.-G.; Kim, M.; Kim, J. *ACS Nano* **2010**, *4*, 2160.
(36) Lynch, J.; O'Neill, L.; Bradley, D.; Byrne, H. J.; McNamara, M. *Macromolecules* **2007**, *40*, 7895.
(37) Gill, R. E.; van Hutten, P. F.; Meetsma, A.; Hadziioannou, G. *Chem. Mater.* **1996**, *8*, 1341.
(38) Shen, P.; Sang, G.; Lu, J.; Zhao, B.; Wan, M.; Zou, Y.; Li, Y.; Tan, S. *Macromolecules* **2008**, *41*, 5716–5722.
(39) Egbe, D. A. M.; Kietzke, T.; Carbonnier, B.; Mühlbacher, D.; Hörhold, H.-H.; Neher, D.; Pakula, T. *Macromolecules* **2004**, *37*, 8863–8873.
(40) Leriche, P.; Raimundo, J.-M.; Turbiez, M.; Monroche, V.; Allain, M.; Sauvage, F.-X.; Roncali, J.; Frère, P.; Skabara, P. J. *J. Mater. Chem.* **2003**, *13*, 1324–1332.
(41) Wang, S.-L.; Ho, T.-I. *J. Photochem. Photobiol. A* **2000**, *135*, 119.
(42) An, B.-K.; Kwon, S.-K.; Jung, S.-D.; Park, S. Y. *J. Am. Chem. Soc.* **2002**, *124*, 14410.
(43) Kim, M.-S.; Kang, M.-G.; Guo, L. J.; Kim, J. *Appl. Phy. Lett.* **2008**, *92*, 133301.
(44) Choulis, S. A.; Kim, Y.; Nelson, J.; Bradley, D. D. C.; Giles, M.; Shkunov, M.; McCulloch, I. *Appl. Phys. Lett.* **2004**, *85*, 3890.
(45) Shrotriya, V.; Yao, Y.; Li, G.; Yang, Y. *Appl. Phy. Lett.* **2006**, *89*, 063505.
(46) Chua, L.-L.; Zaumseil, J.; Chang, J.-F.; Ou, E. C.-W.; Ho, P. K.-H.; Sirringhaus, H.; Friend, R. H. *Nature* **2005**, *434*, 194.
(47) Maurano, A.; Hamilton, R.; Shuttle, C. G.; Ballantyne, A. M.; Nelson, J.; O'Regan, B.; Zhang, W.; McCulloch, I.; Azimi, H.; Morana, M.; Brabec, C. J.; Durrant, J. R. *Adv. Mater.* **2010** (adma.201002360).
(48) Perez, M. D.; Borek, C.; Forrest, S. R.; Thompson, M. E. *J. Am. Chem. Soc.* **2009**, *131*, 9281.
(49) Kim, M.-S.; Kim, B.-G.; Kim, J. *ACS Appl. Mater. Interfaces* **2009**, *1*, 1264.
(50) Berson, S.; Bettignies, R.; Bailly, S.; Guillerez, S. *Adv. Funct. Mater.* **2007**, *17*, 1377.